Acta Crystallographica Section D
Biological Crystallography
ISSN 0907-4449

Structure of the heterodimeric neurotoxic complex viperotoxin F (RV-4/RV-7) from the venom of *Vipera russelli formosensis* at 1.9 Å resolution

Markus Perbandt,[a] Inn-Ho Tsai,[b] Annemarie Fuchs,[a] Sankaran Banumathi,[c] Kanagalaghata R. Rajashankar,[c] Dessislava Georgieva,[a] Narayana Kalkura,[a] Tej P. Singh,[d] Nicolay Genov[e] and Christian Betzel[a]*

[a]Institute of Biochemistry and Molecular Biology I, University Hospital Hamburg-Eppendorf, c/o DESY, Building 22a, Notkestrasse 85, 22603 Hamburg, Germany, [b]Institute of Biological Chemistry, Academia Sinica, PO Box 23-106, Taipei, Taiwan, [c]National Cancer Institute, Frederick and Brookhaven National Laboratory, New York 11973, USA, [d]Department of Biophysics, All India Institute of Medical Sciences, New Delhi 110029, India, and [e]Institute of Organic Chemistry, Bulgarian Academy of Sciences, 'Acad. G. Bonchev' Str. Bl. 9, Sofia 1113, Bulgaria

Correspondence e-mail: betzel@unisgi1.desy.de

Received 1 April 2003
Accepted 4 July 2003

PDB Reference: viperotoxin F, 1oqs, r1oqssf.

The presynaptic viperotoxin F is the major lethal component of the venom of *Vipera russelli formosensis* (Taiwan viper). It is a heterodimer of two highly homologous (65% identity) but oppositely charged subunits: a basic and neurotoxic PLA_2 (RV-4) and an acidic non-toxic component with a very low enzymatic activity (RV-7). The crystal structure of the complex has been determined by molecular replacement and refined to 1.9 Å resolution and an *R* factor of 22.3% with four RV-4/RV-7 complexes in the asymmetric unit, which do not exhibit any local point-group symmetry. The complex formation decreases the accessible surface area of the two subunits by ~1425 $Å^2$. Both PLA_2s are predicted to have very low, if any, anticoagulant activity. The structure of viperotoxin F is compared with that of the heterodimeric neurotoxin vipoxin from the venom of another viper, *V. ammodytes meridionalis*. The structural basis for the differences between the pharmacological activities of the two toxins is discussed. The neutralization of the negative charge of the major ligand for Ca^{2+}, Asp49, by intersubunit salt bridges is probably a common mechanism of self-stabilization of heterodimeric Viperinae snake-venom neurotoxins in the absence of bound calcium.

1. Introduction

Phospholipase A_2s (PLA_2s; phosphatide 2-acylhydrolases; EC 3.1.14) are intracellular or extracellular enzymes that hydrolyze the 2-acyl ester bond of 1,2-diacyl-3-*sn*-phosphoglycerides, thereby releasing fatty acids and lysophospholipids. Some of them are single-chain proteins, but others can form multicomponent structures. Snake-venom extracellular PLA_2s vary considerably in their quaternary structure and exist as monomers, homodimers or heterodimers or multichain aggregates (Bon, 1997). They display a variety of pharmacological activities such as presynaptic/postsynaptic neurotoxicity, myotoxicity, cardiotoxicity and anticoagulant, antiplatelet, convulsant, hypotensive, haemolytic, haemorrhagic and oedema-inducing effects (Huang *et al.*, 1997). Russell's viper (*Vipera russelli*) is the major cause of fatal snakebites in southeast Asia, resulting in more than 1000 deaths per year (Maung-Maung-Aye, 1990; Maung-Maung-Thwin *et al.*, 1995). The heterodimeric neurotoxin viperotoxin F is the major lethal component of the venom of *V. russelli formosensis* (Taiwan viper). It represents a complex between a neurotoxic and enzymatically active basic PLA_2 (termed RV-4) and a non-toxic acidic PLA_2 (RV-7), which has a 100-fold lower hydrolytic activity than that of RV-4 (Wang *et al.*, 1992). Both components of viperotoxin F are highly homologous proteins and their amino-acid sequences share 65% identity. It can be supposed that RV-7 is a product of evolution

of RV-4 and *vice versa*. The targets of the Taiwan viper toxin are the presynaptic sites of the neuromuscular junctions, which lead to a blockade of the breathing muscles and to rapid death. The non-toxic PLA_2 also plays an important pharmacological role. It potentiates the lethal effect and neuromuscular blocking activity of RV-4 by up to threefold. At the same time, upon complex formation the enzymatic activity of the toxic subunit towards both micellar and monomeric substrates is 40–60% reduced by RV-7 (Wang *et al.*, 1992).

It is remarkable that viperotoxin F from the Taiwan (Asia) viper is closely related to the neurotoxic complex vipoxin from the Bulgarian (southeast Europe) sand viper *V. ammodytes meridionalis* venom. *V. russelli formosensis* is a medically important Viperinae snake that only inhabits the island of Taiwan (Tsai *et al.*, 1996). On the other hand, *V. ammodytes meridionalis* is widespread in the central part of the Balkan peninsula (Aleksiev & Shipolini, 1971). Both neurotoxins are similar in primary structure but differ in their mode of biological action. Viperotoxin F is a presynaptic toxin (Wang *et al.*, 1992), while vipoxin is postsynaptic (Mancheva *et al.*, 1986); *i.e.* the place of physiological attack is changed. The non-toxic component of the neurotoxin from *V. russelli formosensis*, RV-7, potentiates the PLA_2 toxicity. However, its counterpart from vipoxin (Inh) acts as an inhibitor, decreasing the toxicity of the PLA_2 subunit by fivefold. Finally, in contrast to RV-7, which possesses weak phospholipase A_2 activity, the vipoxin inhibitor is catalytically inactive (Aleksiev & Chorbanov, 1976). The N-terminal sequence of the single-chain daboiatoxin, the major lethal component of the venom of the Burmese Russell's viper (*Daboia russelli siamensis*), is highly homologous to the two PLA_2s of viperotoxin F and both components of vipoxin (Maung-Maung-Thwin *et al.*, 1995).

Here, we describe the structure of viperotoxin F refined to 1.9 Å resolution. The three-dimensional model reveals the structural features that are responsible for the formation of a complex between the two different PLA_2 molecules, leading to an increase in the toxicity. In the absence of bound Ca^{2+}, the complex is stabilized by two intersubunit salt bridges. The inhibitory effect of RV-7 is also explained, which is important from a pharmacological point of view. We have recently published the high-resolution (1.4 Å) structure of vipoxin (Banumathi *et al.*, 2001). The present structure allows a comparison of two heterodimeric neurotoxic complexes, viperotoxin F and vipoxin, which differ in their targets of physiological attack and in several other properties. Comparison of the two structures permits prediction and explanation of the differences in the pharmacological activities of the two neurotoxins.

2. Materials and methods

Crude venom was obtained from the toxic glands of *V. russelli formosensis*. The isolation and crystallization of the neurotoxic complex viperotoxin F were performed as described by Rajashankar *et al.* (1999). In brief, crystals were grown by the hanging-drop vapour-diffusion method at 289 K from 4 µl drops containing 2 µl of 24 mg ml^{-1} protein in 50 m*M* sodium acetate buffer pH 4.5 and 2 µl of the reservoir solution. The drops were equilibrated against 300 µl reservoir solution containing 7% MPD, 1% PEG 4000 and 1 m*M* $CaCl_2$ pH 4.5. After 45 d, a crystal appeared in one of the drops. The remaining drops were clear without crystals. Crystals suitable for X-ray analysis were obtained by applying the seeding technique. The end of a fibre was used to touch the grown crystal and dislodge seeds from it and to introduce seeds into pre-equilibrated clear drops by rapidly moving the fibre in a straight line across the middle of the protein-precipitant drop. The seeds grew to diffraction-quality crystals within 24 h. The space group was assigned as $P2_1$ and the unit-cell parameters were a = 74.92, b = 85.13, c = 78.16 Å, β = 95.12°. There are four molecules of the dimeric complex in the asymmetric unit. Diffraction data to 1.9 Å resolution were collected at beamline X11 (EMBL/DESY, Hamburg) equipped with a MAR Research image-plate scanner. The X-ray wavelength was 0.9063 Å. The images were processed using the programs *DENZO* and *SCALEPACK* (Otwinowski & Minor, 1997). The phase problem was solved by molecular-replacement techniques using the 1.4 Å structure of the neurotoxin vipoxin (Banumathi *et al.*, 2001) as a search model and applying the program *AMoRe* (Navaza, 1994). The vipoxin model was further modified using the rotamer database of the program *O* (Jones *et al.*, 1991). Initial refinement using the program *REFMAC* (Murshudov *et al.*, 1997) and data between 25 and 1.9 Å reduced the R factor to 35.7% (Table 1). For all the following calculations the *CCP*4 program suite (Collaborative Computational Project, Number 4, 1994) was applied and for model building the program *TURBO-FRODO* (Roussel & Cambillau, 1991) was used. The solvent molecules were added subsequently during refinement at chemically reasonable

Table 1
Data-collection and refinement statistics.

Values in parentheses are for the last resolution shell.

Space group	$P2_1$
Unit-cell parameters (Å, °)	a = 74. 92 b = 85. 13, c = 78.16, β = 95.12
V_M (Å^3 Da^{-1})	2.22
Wavelength used (Å)	0.9063
Data collection and refinement	
Resolution (Å)	25–1.9 (1.95–1.90)
No. of unique reflections	74210
R_{merge} (%)	6.1 (28.1)
Completeness (%)	98.1 (97.9)
Refinement statistics	
R value/R_{free} (%)	21.7/27.7
No. of amino acids	976
No. of solvent molecules	359
Average B factors (Å^2)	
Protein	25.2
Water molecule	26.6
R.m.s. deviations from ideal value	
Bond distances (Å)	0.028
Bond angle (°)	2.469
Torsion angles (°)	5.133
Ramachandran plot: non-Gly residues in	
Most favoured regions (%)	87.8
Additionally allowed regions (%)	11.2
Generously allowed regions (%)	1.0
Disallowed regions (%)	0
Luzzati coordinate error (Å)	0.185

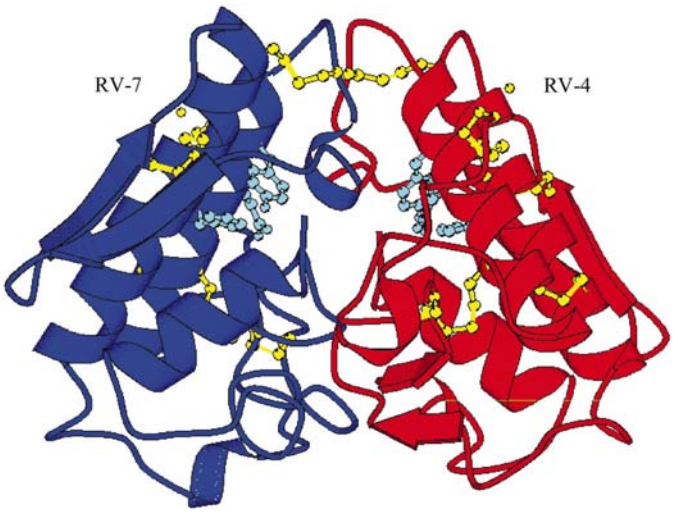

Figure 1
Ribbon representation of viperotoxin F from the venom of *V. russelli formosensis*. The toxic subunit RV-4 is coloured red and the non-toxic RV-7 blue. The disulfide bridges and active-site residues are shown as ball-and-stick models in yellow and cyan, respectively. The figure was generated using the program *MOLSCRIPT* (Kraulis, 1991).

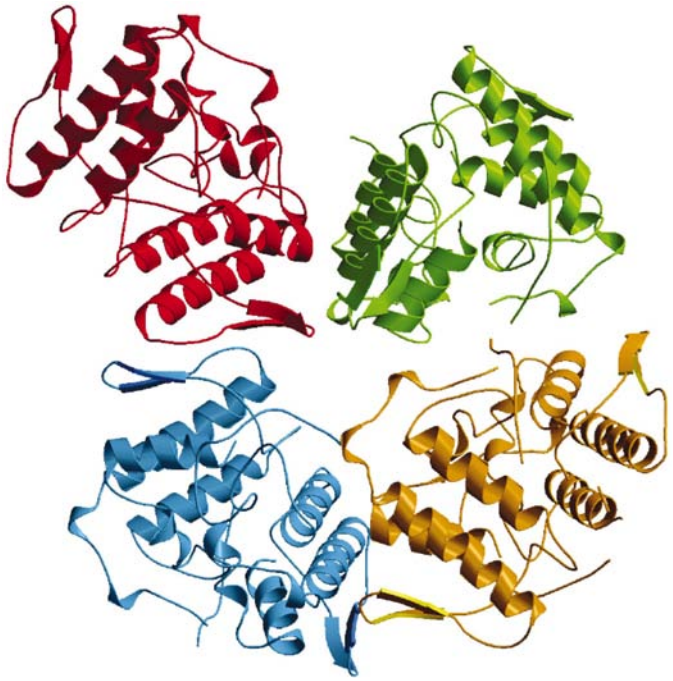

Figure 2
Interaction and arrangement of the RV4/RV7 heterodimers, shown in different colours, in the asymmetric unit.

positions where difference density exceeded 3σ. The quality of the model was checked using the program *PROCHECK* (Laskowski *et al.*, 1993).

3. Results and discussion

3.1. Description of the overall structure of viperotoxin F

The refined model of viperotoxin F at 1.9 Å resolution consists of 9797 non-H atom positions and 359 water molecules. Data-collection and refinement statistics are shown in Table 1. The neurotoxic complex is globularly shaped (Fig. 1) and has dimensions of ~30 × 35 × 55 Å. Viperotoxin F is composed of two subunits with similar folding. Each monomer has dimensions of approximately 15 × 30 × 35 Å. The secondary-structure elements of the respective subunit include three α-helices and a specific β-wing structure (residues 74–85), which is a segment of a β-sheet structure. Two long helices, Ala40–Gly54 (Thr54 in RV-7) and Ala89 (Asp89 in RV-7)–Asn109, are antiparallel and form one of the walls of the substrate-binding pocket. The mutual orientation of these helices is fixed by two disulfide bonds, Cys44–Cys105 and Cys51–Cys98. The third α-helix includes the N-terminal part of the polypeptide chain (residues Leu2–Gly14). The β-wing includes residues Ser74–Gly85 (Asp85 in RV-7) and represents a single loop of antiparallel β-sheet. This substructure is conserved in all class I/II PLA_2s (Scott, 1997). The disulfide

Table 2
Intermolecular contacts.

(*a*) Direct intermolecular contacts between complexes in the asymmetric unit.

		Distances (Å)
AB	*CD*	
Glu78*A* O	Arg129*D* NH2	2.53
	EF	
Leu10*A* O	Arg100*F* NH2	3.08
Gln11*A* OE1	Arg100*F* NH1	3.26
Gln11*A* NE2	Asn81*F* OD1	2.72
Glu78*A* OE1	Arg79*F* NH1	3.39
Glu78*A* OE2	Arg79*F* NH1	3.25
Asn79*A* N	Arg79*F* O	2.63
Gly107*A* O	Gln108*F* NE2	2.63
CD	*GH*	
Gln108*D* NE2	Glu11*G* OE1	2.65
Gln108*D* O	Gly80*G* N	3.00
Asn111*D* ND2	Asn79*G* OD1	3.03
Cys133*D* OXT	Lys115*G* NZ	2.78
EF	*GH*	
Asn116*E* ND2	Gly11*H* O	3.27
Ser124*E* O	Arg7*H* NH2	2.53
Arg7*F* NH2	Ser124*G* O	2.63
Gly11*F* O	Asn116*G* ND2	3.30

(*b*) Intermolecular contacts stabilizing the viperotoxin F complex. Data extracted from the dimer with chain identifiers *A* and *B*.

RV-7	RV-4	Distances (Å)
Asn1 ND2	Gln34 OE1	2.98
Leu2 N	Gly32 O	3.05
Phe3 N	Gly32 O	3.13
Tyr28 O	Lys69 NZ	2.88
Trp31 O	Phe3 N	3.27
Tyr28 O	Lys69 NZ	2.88
Gly32 O	Phe3 N	2.95
Gly32 O	Leu2 N	3.21
Gly33 O	Asn1 ND2	3.36
Asn34 OE1	Asn1 ND2	2.99
Asp49 OD1	Lys69 NZ	2.80
Asp49 OD2	Lys69 NZ	2.73
Asp49 O	Asn61 ND2	3.04
Asn56 O	Lys56 NZ	3.09
Asn61 ND2	Asp49 O	3.10
Lys69 NZ	Gly30 O	2.94
Lys69 NZ	Asp49 OD1	3.23
Lys69 NZ	Asp49 OD2	3.23

bond Cys84–Cys96 connects the flexible β-wing, which is important for the toxicity, with an α-helix. The structure of each subunit is further stabilized by the disulfide bonds Cys59–Cys91, Cys50–Cys133, Cys27–Cys126 and Cys29–Cys45. The asymmetric unit contains four complexes. They are arranged like a four-leaved clover (Fig. 2). The conformations of the four complexes are almost identical and their superposition showed an r.m.s. deviation of 0.34 Å including all C^{α} atoms. The conformations of the β-wings is practically conserved for the four protomers, with maximum r.m.s. values of 0.16 Å which is inside the expected overall coordinate error at this resolution. The intermolecular contacts between the heterodimers in the asymmetric unit and the intersubunit contacts, which stabilize the neurotoxic complex, are summarized in Table 2(*a*) and 2(*b*), respectively. Comparison of the published amino-acid sequence of the complex RV-4/RV-7 (Wang *et al.*, 1992) and that from the X-ray data revealed some differences. In the RV-4 chain the differences are Lys56Arg, Asn89Ala, Glu116Asn and Gln132Lys, and in RV-7 they are Leu90Ser and Gln132Ser. In the present manuscript, we use the sequence from the crystallographic model. Fig. 3 shows the location of the catalytic site and the putative neurotoxic and anticoagulant sites in the toxic RV-4.

3.2. Catalytic site and hydrophobic channel

The catalytic site of each subunit of viperotoxin F is located at the bottom of a hydrophobic channel built up of residues Leu2, Phe5, Met8, Ile9, Tyr22, Cys29, Lys69, Ala 102, Ala103 and Phe106 (Leu106 in RV-7). This channel accommodates the acyl portion of the substrate. In the absence of a substrate, the hydrophobic cleft is occupied by water molecules, which is characteristic for the class I/II secretory PLA_2s (Scott, 1997). The catalytic site consists of the triad His48–Asp99–water, along with Tyr52 and Tyr73 (Fig. 4). Although similar in three-dimensional structure, the two components of viperotoxin F differ considerably in catalytic activity. Both subunits are Asp49 PLA_2s. However, the enzyme activity of RV-7 toward micellar and monomeric substrates is about 100-fold lower than that of RV-4 (Wang *et al.*, 1992). The catalytic site, hydrophobic channel and calcium-binding loop 25–33 are preserved in RV-7. The acidic components of the snake-venom heterodimeric neurotoxins play the role of chaperones to avoid non-specific binding of the toxic PLA_2 to the target membrane. In the presence of aggregated lipid substrates, the heterodimer dissociates into subunits. Only the basic subunit binds to the substrate and exerts toxicity (Bon, 1997). The second, acidic, component remains in solution and there is no biological necessity for this subunit to be catalytically active or toxic. The low level of enzymatic activity of RV-7 may be attributed to the five acidic amino-acid residues in positions 7, 17, 59, 114 and 119, which probably impair its binding to the negatively charged lipid substrates because of electrostatic repulsions (Wang *et al.*, 1992). Table 3 demonstrates the predominant number of positively charged residues in the toxic RV-4 and

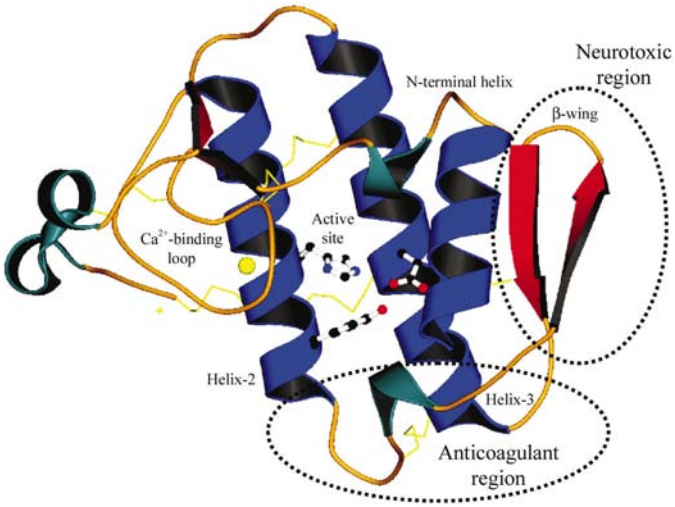

Figure 3
Cartoon representation of the viperotoxin F subunit RV-4. The active-site residues are presented as ball-and-stick models. The putative anticoagulant and neurotoxic regions are also shown. The figure was generated using the program *MOLSCRIPT* (Kraulis, 1991).

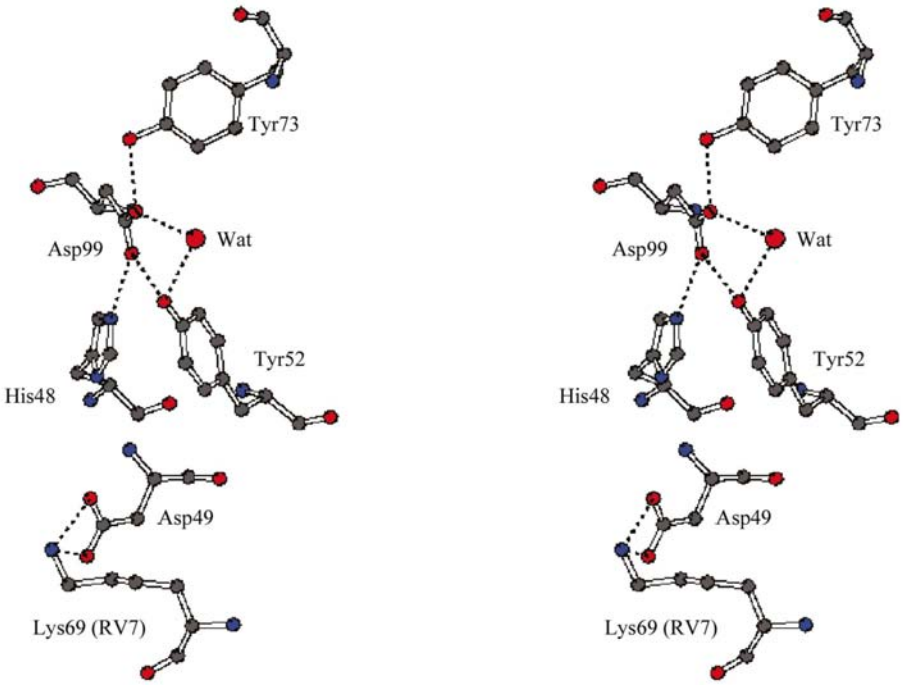

Figure 4
Stereofigure showing the active-site residues of RV-4 from viperotoxin F and the salt bridge between RV-4 Asp49 and RV-7 Lys69 that stabilizes the complex.

Table 3
Charged residues at pH 6–7, not including the C- and N-termini and aromatic residues of viperotoxin F, compared with vipoxin PLA_2 and Inh (Vipo; PDB code 1jlt), the PLA_2s from *Crotalus atrox* (PDB code 1pp2) and *Agkistrodon halys pallas* (agkistrodotoxin; ATX; PDB code 1a2a).

			Vipo			
	RV-4	RV-7	PLA_2	Inh	*C. atrox*	ATX
Arg (+)	8	4	7	5	4	6
Asp (−)	4	7	5	10	10	7
Glu (−)	3	10	2	8	8	10
Lys (+)	8	4	9	4	6	9
Total	23	25	23	27	28	32
Positive	16	8	16	9	10	15
Negative	7	17	7	18	18	17
Salt bridges			7	7	7	7
Trp	2	1	2	1	3	0
Tyr	8	10	8	10	8	10
Phe	7	4	7	4	4	6
SA† (Å^2)	7085	7604	7432	7115	7147	6965
SA, dimer (Å^2)	11776		11586		11787	12085

† Surface accessibility.

related components of heterodimeric snake-venom neurotoxins compared with their acidic counterparts.

3.3. Self-stabilization of the complex in the absence of bound calcium

Ca^{2+} is essential for Asp49 PLA_2s because it stabilizes the tetrahedral intermediate with the substrate (Scott *et al.*, 1992). The calcium-binding loop is formed by residues 25–33 and the coordination sphere includes the carboxylic group of Asp49, the backbone carbonyl O atoms of residues 28, 30 and 32, and two water molecules (Scott, 1997). However, no bound calcium ion was observed at the putative metal ion-binding sites of either RV-4 or RV-7 because the crystallization was performed in the presence of 1 m*M* $CaCl_2$, which proved to be insufficient for saturation of the metal ion-binding site. The conformation of this region is quite different from that of other Asp49 PLA_2s with bound Ca^{2+} and the mutual orientation of the possible ligands is not suitable for coordination of the calcium ion. In the neurotoxic complex from *V. russelli formosensis*, the ε-amino group of Lys69 from the subunit RV-7 neutralizes the negative charge of the RV-4 Asp49 (Fig. 4) and *vice versa*. The carboxylic groups of the Asp49 residues are the major charged ligands of Ca^{2+}. The positively charged ε-NH_2 simulates the role of the divalent cation. In this way, the apparent flexibility of the calcium-binding loop is neutralized by two intersubunit salt bridges and the local substructure is sufficiently stabilized. In Fig. 5, the metal ion-binding region of the Ca^{2+}-free RV-4 is compared with that of the *Naja naja atra* PLA_2 (PDB code 1pob) as a representative of the calcium-dependent phospholipase A_2s with bound metal ions.

3.4. PLA_2–PLA_2 complex formation

The complex between the two PLA_2s of viperotoxin F is formed through ionic, hydrophobic and hydrogen-bonding interactions. RV-4 is a basic protein with a pI of 10.0, while RV-7 is acidic and has a pI of 4.3 (Wang *et al.*, 1992). This creates a strong electrostatic attraction between the two oppositely charged molecules. Figs. 6(*a*) and 6(*b*) show the surface potentials of the two subunits and the electrostatic differences are obvious. The salt bridges between the Asp49 residues and Lys69 mentioned above additionally stabilize the heterodimer. Inspection of the model showed that hydrophobic forces are also important for complex formation. The two tryptophans of RV-4 and the single indole group of RV-7 are 'buried' in the intersubunit region and participate in strong hydrophobic interactions that stabilize the conformation of the complex. The model reveals a number of inter-chain hydrogen bonds between backbone carbonyl O atoms of RV-4 and side-chain atoms of RV-7 (Table 2*b*). Complex formation decreases the accessible surface area of the two PLA_2s by ∼1420 Å^2, which results in a decrease of the RV-4 enzymatic

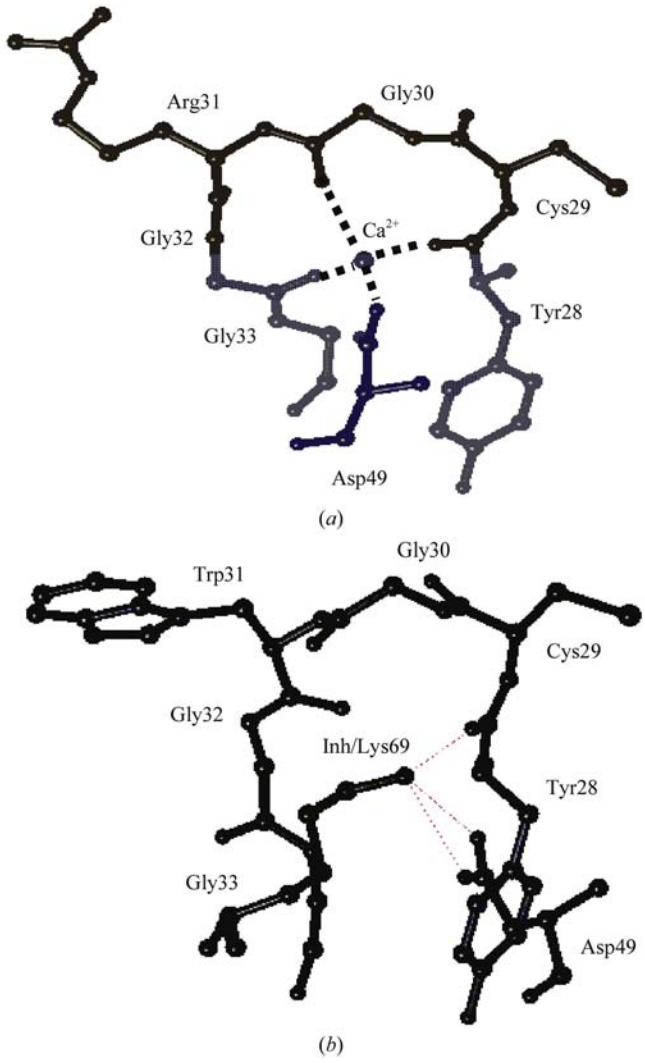

Figure 5
Ball-and-stick representation of the calcium-binding sites of *N. naja atra* PLA_2 (PDB code 1pob) with bound calcium (*a*) and the Ca^{2+}-free RV-4 from viperotoxin F (*b*). The metal ion is coordinated by the carboxylate group of Asp49 and three backbone O atoms as indicated in the figure. The conformation of the loop in RV-4 is slightly changed.

activity. The X-ray structure of viperotoxin F shows that RV-7 partially blocks the entrance of the hydrophobic channel that accommodates the acyl portion of the substrate. This may explain the reduction of hydrolytic activity upon dimer formation.

3.5. Interfacial adsorption surface

Secreted PLA_2s catalyze the hydrolysis of natural substrates at the lipid–water interface (interfacial catalysis), which explains their preference for aggregates such as membranes or mixed micelles and their considerably lower activity towards dispersed lipids. The catalytic activity depends on the adsorption of the enzyme on the water–lipid interface. The interfacial adsorption surface (IAS) of snake-venom PLA_2s envelops and incorporates the external opening of the hydrophobic channel (Scott, 1997), which is exposed to the solvent. The IAS of RV-4 from viperotoxin F includes Ala6, Arg7, Asn10, Phe17, Ser18, Val19, Trp20, Asn21, Ile23, Ser24, Lys69, Leu70, Ile72, Tyr116, Lys117, Ser123 and Lys124. Residues in these positions participate in the IASs of other class I/II PLA_2s (Heinrikson & Kezdy, 1990), but the nature of their surfaces is quite variable. The adsorption surface includes part of the N-terminal helix and lies almost perpendicular to the channel, which is surrounded by hydrophobic amino-acid residues. The surface is responsible for the adsorption of the toxin onto the membrane–water interface. Apart from hydrophobic side chains, it contains four basic residues that should be important for interfacial catalysis. It has been shown (Han *et al.*, 1997) that electrostatic interactions are essential for this type of catalysis. The basic residue in position 7 plays an especially important role in the adsorption of PLA_2 to anionic surfaces. Comparison of the adsorption surfaces of the two subunits of viperotoxin F shows that, with several exceptions, all the other residues in the nontoxic RV-7 are substituted, including the important Arg7, *i.e.* Ala6Gly, Arg7Glu, Asn10Leu, Phe17Glu, Ser18Val, Trp20His, Asn21Ser, Ile23Ala, Ser24Ile, Leu70Thr, Ile72Thr and Lys124His. Three of the four basic residues are substituted, two of them by acidic residues. As a result of these substitutions, the net positive charge of the adsorption surface of the toxic and catalytically active RV-4 is changed to a net negative charge in the corresponding region of RV-7, which is nontoxic and almost inactive towards micellar and monomeric substrates. The electrostatic interactions between the positive charges from the enzyme adsorption surface and negatively charged phospholipids are known to be important for the efficiency of catalysis (Scott, 1997). Most probably, the drastic difference in the charge of the IASs in the two subunits is one of the major reasons for the loss of hydrolytic activity and toxicity of one of them (RV-7).

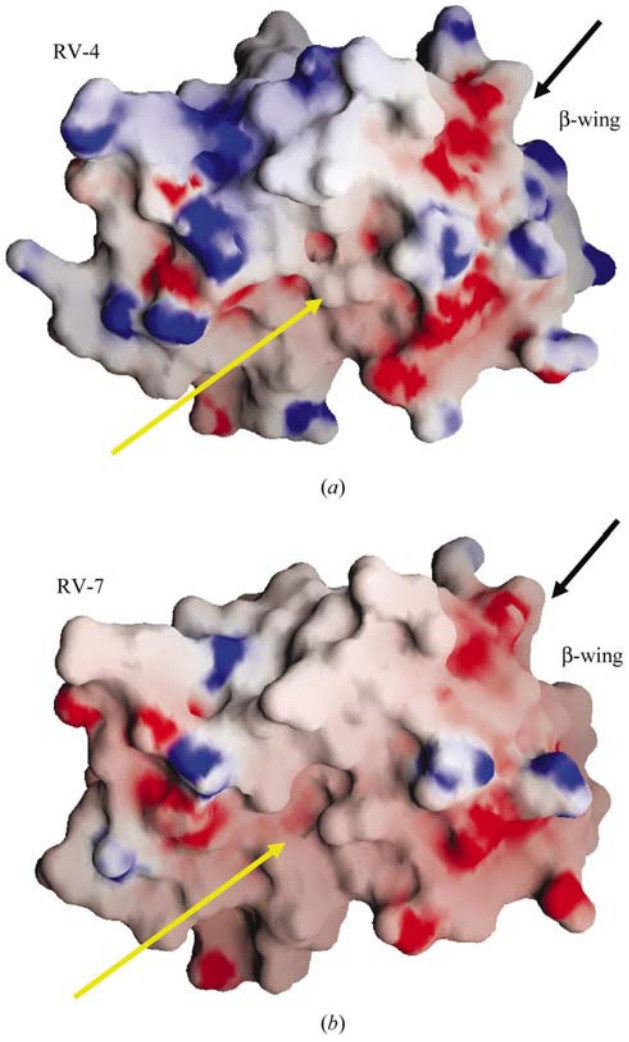

Figure 6
Surface potential of viperotoxin F, prepared using the program *GRASP* (Nicholls *et al.*, 1991). Positive charges are indicated in blue and negative charges in red. (*a*) RV-4, (*b*) RV-7. The active-site region is indicated by a yellow arrow and the β-wing region by a black arrow.

3.6. Pharmacologically important sites

3.6.1. Anticoagulant site. PLA_2s from Viperidae snake venoms can exert different effects on blood coagulation (Evans & Kini, 1997). Some of them are strongly anticoagulant (Boffa *et al.*, 1972; Teng *et al.*, 1984), while others exert weak or non-anticoagulant effects. Usually, basic group II PLA_2s show anticoagulant activity (Verheij *et al.*, 1980). This pharmacological activity is connected to a site in the PLA_2 molecule consisting of residues 53–77. The most important part of this site is a cationic surface formed by the side chains of four positively charged residues. This site binds anionic phospholipids during the anticoagulation process (Kini & Evans, 1989; Mounier *et al.*, 1996, 1998). In the weakly or non-anticoagulant PLA_2s, two or more of the basic residues from the anticoagulant sites are replaced with neutral or acidic residues (Evans & Kini, 1997). The structure of viperotoxin F shows the presence of two basic residues, Arg56 and Lys69, in the putative anticoagulant site of RV-4. Only Lys69 is preserved in the respective region of RV-7. Arg54 is conserved in all known group II PLA_2s (Zhao *et al.*, 2000) and the two enzymes of viperotoxin F are, to our knowledge, the only exception to this rule reported so far. Position 54 is occupied by a glycine in RV-4 and a threonine in RV-7. It was suggested

that a glutamic acid in position 53 may be important for anticoagulant activity (Carredano *et al.*, 1998). However, in both RV-4 and RV-7 this position is occupied by glycine. Therefore, it can be predicted that the two subunits will lack or will have a very low anticoagulant activity.

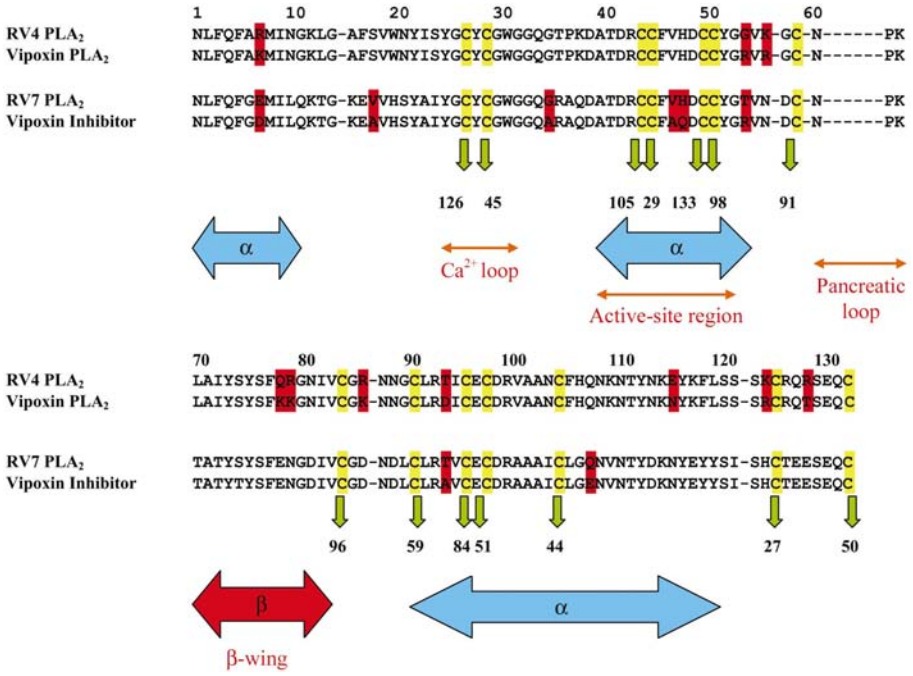

Figure 7
Comparison of the amino-acid sequences of viperotoxin F from the Taiwan (Asia) viper *V. russelli formosensis* and vipoxin from the European sand viper *V. ammodytes meridionalis* (Mancheva *et al.*, 1987). The basic and acidic components of viperotoxin F are 92% identical to their counterparts from vipoxin. The differences in the sequences are shown in red. The sequence numbering is in accordance with the literature; the accepted reference is the structure of bovine pancreatic PLA_2. The regions of secondary structure, catalytic and functional sites, residues involved in potential calcium binding and the so-called pancreatic loop found only in the group I PLA_2s are indicated below accordingly. Cysteines are shown with the sequence number of their disulfide counterpart.

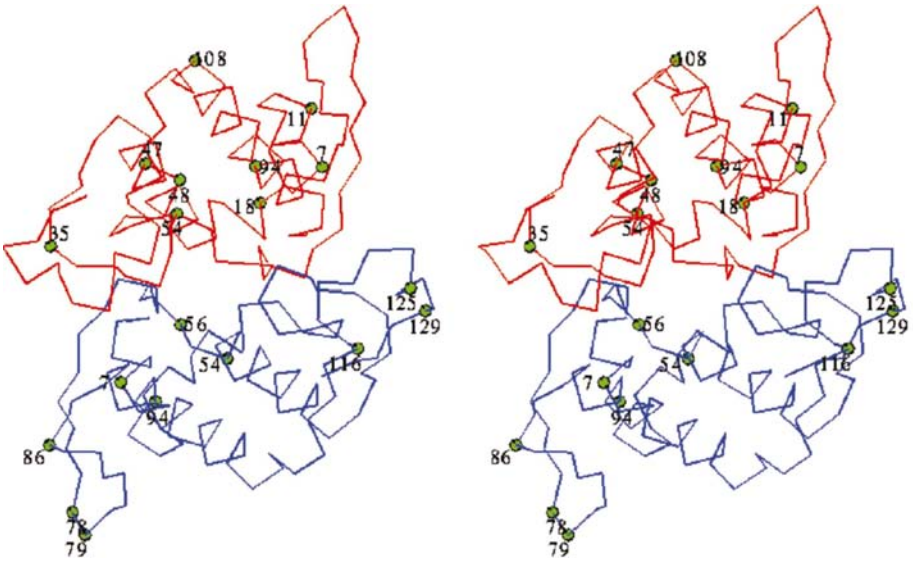

Figure 8
Stereoview of viperotoxin (RV4, blue; RV7, red); positions where amino acids change in comparison to vipoxin are labelled.

3.6.2. Neurotoxic site. The neurotoxicity of viperotoxin F arises from specific binding and hydrolysis at sites on presynaptic membranes that are critical for transmitter release. As mentioned previously, the heterodimer consists of a toxic basic component (RV-4) and a nontoxic acidic component (RV-7). Acidic snake-venom PLA_2s alone are not toxic (Krizaj *et al.*, 1996), but for the most part the basic ones are. However, the nontoxic subunit potentiates the neurotoxicity of RV-4, which suggests a chaperone function of RV-7 that prevents non-specific binding of the toxic enzyme to other targets (lipid sites) different from presynaptic membranes. The toxicity site of RV-4 is built up by the side chains of residues 6, 12, 76–81 and 119–125 (Wang *et al.*, 1992). It was subsequently shown that almost the entire C-terminal region, 119–129, is important for the membrane-damaging activity of snake-venom PLA_2s (Lomonte *et al.*, 1999). The model of RV-4 shows that the residues of the toxicity site are located on the protein surface and can interact with receptors. The segment 74–85 is, in principle, a flexible β-wing structure. The flexibility of this part of the polypeptide chain is probably important for the interactions with membranes. Electrostatic effects between positively charged residues from the toxicity site of PLA_2 and negatively charged regions of the presynaptic membranes may play an important role in the binding to and subsequent damage to the natural substrates. Aromatic residues are also important in this process (Lomonte *et al.*, 1999; Sumandea *et al.*, 1999). Comparison of the structures of the two components of viperotoxin F shows a number of substitutions in the region of the toxicity site, leading to a drastic change of the electrostatic charge from positive in RV-4 to negative in RV-7. The β-wing of the first subunit is positively charged, while the same structure in the second subunit has a negative charge (Fig. 6). The C-terminal parts of the two PLA_2s of the complex also have opposite charges: positive in the case of RV-4 (four basic residues) and strongly negative in RV-7 (four acidic side chains). Taken together, these changes in the electrostatic charge of the region in RV-7 that corresponds to the toxicity

site in RV-4 are the most probable reason for the lack of toxicity in RV-7.

3.7. Comparison of the structures of viperotoxin F and vipoxin

The sequences of the two subunits of viperotoxin F from the Taiwan viper are 92% identical to those of the respective components of vipoxin from the venom of the European viper *V. ammodytes meridionalis* (Fig. 7). As shown in Fig. 8, the changes in the sequence are located entirely on the surface of the heterodimer. From a functional point of view, the most important differences between the heterodimeric neurotoxins from the two Viperinae snakes are connected with their pharmacological activities. One of the purposes of the present work is to find the structural basis of the functional differences between the two closely related neurotoxic complexes. The C^{α} positions of the basic toxic components were superimposed with an r.m.s. difference of 0.35 Å and a maximum displacement of 2.69 Å (Fig. 9*a*). The respective values for the pair of non-toxic subunits are 0.47 and 1.82 Å (Fig. 9*b*). The comparison of the structures of viperotoxin F and vipoxin demonstrates a complete conservation of secondary-structure elements. The major differences between RV-4 and the vipoxin PLA_2 are in the putative anticoagulant site and in regions connected with toxicity: the β-wing and the C-terminal part of the polypeptide chain (Fig. 9*a*). This indicates functional flexibility of the regions mentioned above. There is one important substitution in the β-wing, Gln78Lys, which leads to a change in the electrostatic charge. The differences in the conformation and the charge of the toxicity site are probably connected with the changed position of physiological attack: from the postsynaptic (vipoxin) to the presynaptic (viperotoxin F) membranes of the neuromuscular junctions.

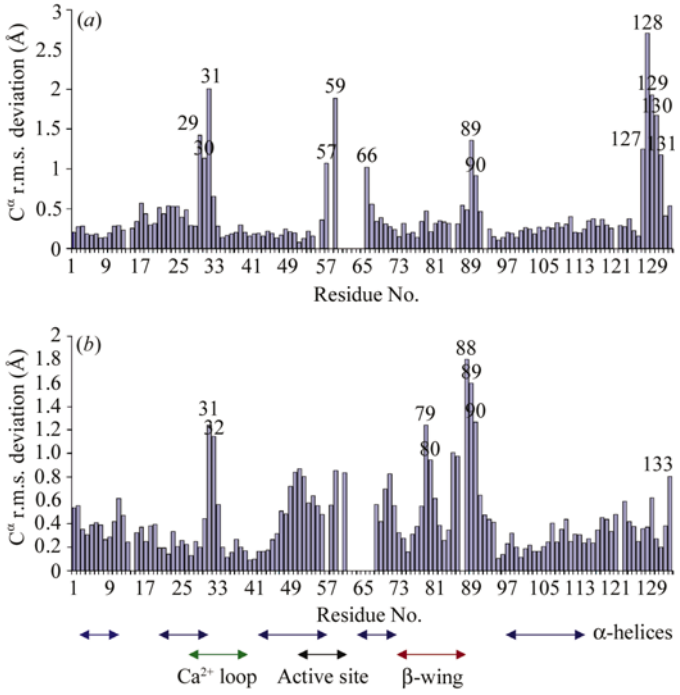

Figure 9
C^{α} r.m.s. plot between vipoxin PLA_2 and RV4 (*a*) and between RV7 and the vipoxin inhibitor (*b*). On the *x* axis the α-helices are indicated by arrows; the Ca^{2+}-loop, active-site and β-wing regions are labelled accordingly.

Comparison of the structures of the two neurotoxins allows the prediction of differences in their anticoagulant properties. As mentioned previously, the major conformational differences between RV-4 and the vipoxin PLA_2 are in the region of the anticoagulant site. As discussed in a previous paragraph, viperotoxin F is most probably devoid of or possesses a very low level of anticoagulant activity because of the reduced number of positively charged residues in its pharmacologically relevant site in comparison to typical anticoagulant PLA_2s. In contrast, vipoxin PLA_2 contains a cluster of three positively charged residues in the region 54–77: Arg54, Arg56 and Lys69. The X-ray model shows that the side chains of these residues are exposed on the protein surface and they can interact with phospholipids. It may then be predicted that the neurotoxin from *V. ammodytes meridionalis* will possess anticoagulant activity.

A comparison of the C^{α} positions of the acidic non-toxic subunits shows differences in the segment of the polypeptide chain including residues 54–100 (β-wing structure and part of an α-helix) (Fig. 9*b*). The putative anticoagulant site and part of the toxicity site are located in corresponding regions of the toxic chains. The vipoxin inhibitor and RV-7 of viperotoxin F differ in their catalytic activity and the effect exerted on the toxic subunit. The first protein lacks the catalytically important His48 (Fig. 7) and this is the reason for the absence of enzymatic activity. In contrast to the vipoxin inhibitor, RV-7 amplifies the neurotoxicity of RV-4, which suggests a chaperone function for the non-toxic PLA_2. This peculiarity is probably connected with differences in the interactions between the toxic and non-toxic subunits of the two heterodimeric complexes. Both acidic components lack neurotoxicity and one of the most probable reasons for this is the drastic change of the electrostatic charge in comparison to that of the toxic PLA_2s of the complexes. In principle, viperotoxin F and vipoxin show the same type of intermolecular stabilization *via* the ε-NH_2 of Lys69 and the negative charge of the major Ca^{2+} ligand, the carboxylic group of Asp49 (Fig. 4). This is probably a common mechanism for stabilization of heterodimeric Viperinae snake-venom neurotoxins in the absence of bound Ca^{2+}.

4. Conclusions

The X-ray structure of the heterodimeric PLA_2 from *V. russelli formosensis* reveals important structure–function relationships and allows comparison of the structures of two closely related neurotoxic complexes, viperotoxin F and vipoxin. It was possible to explain and predict the differences in the pharmacological activities of these toxins. The structures of the two complexes demonstrate similar folding of the polypeptide chains. The high degree of sequence and three-dimensional structural similarities among the basic as well as the acidic components of the heterodimeric Viperinae snake-

venom neurotoxins suggest that they are most probably products of evolution from a common ancestor.

The authors thank the Deutsche Forschungsgemeinschaft for financial support from Project 436 BUL 113/115/01 and BE 1443/9-1. DG thanks the Alexander von Humboldt Foundation, Bonn, Germany for providing a Research Fellowship. This project was further supported by a joint grant from the DAAD (Deutscher Akademischer Austauschdienst, Germany) and by a grant from the Department of Science and Technology (DST), New Delhi in terms of the Project Based Personnel Exchange Programme 2000.

References

Aleksiev, B. & Chorbanov, B. (1976). *Toxicon*, **14**, 477–484.
Aleksiev, B. & Shipolini, R. (1971). *Hoppe-Seyler's Z. Physiol. Chem.* **352**, 1183–1187.
Banumathi, S., Rajashankar, K. R., Noetzel, C., Aleksiev, B., Singh, T. P., Genov, N. & Betzel, Ch. (2001). *Acta Cryst.* D**57**, 1552–1559.
Boffa, M. C., Delori, P. & Soulier, J. P. (1972). *Thromb. Diath. Haemorrh.* **28**, 509–523.
Bon, C. (1997). *Venom Phospholipase A_2 Enzymes: Structure, Function and Mechanism*, edited by R. M. Kini, pp. 269–286. Chichester: John Wiley & Sons.
Carredano, E., Westerlund, B., Persson, B., Saarinen, M., Ramaswamy, S., Eaker, D. & Eklund, H. (1998). *Toxicon*, **36**, 75–92.
Collaborative Computational Project, Number 4 (1994). *Acta Cryst.* D**50**, 760–763.
Evans, H. J. & Kini, R. M. (1997). *Venom Phospholipase A_2 Enzymes: Structure, Function and Mechanism*, edited by R. M. Kini, pp. 353–368. Chichester: John Wiley & Sons.
Han, S. K., Yoon, E. T., Scott, D. L., Sigler, P. B. & Cho, W. (1997). *J. Biol. Chem.* **272**, 3573–3582.
Heinrikson, R. L. & Kezdy, F. J. (1990). *Adv. Exp. Med. Biol.* **279**, 37–47.
Huang, M. Z., Gopalakrishnakone, P., Chung, M. C. M. & Kini, R. M. (1997). *Arch. Biochem. Biophys.* **338**, 150–156.
Jones, T. A., Zou, J. Y., Cowan, S. W. & Kjeldgaard, M. (1991). *Acta Cryst.* A**47**, 110–119.
Kini, R. M. & Evans, H. J. (1989). *Toxicon*, **27**, 613–635.
Kraulis, P. J. (1991). *J. Appl. Cryst.* **24**, 946–950.
Krizaj, I., Bdolah, A., Gubensek, F., Bencina, P. & Pungercar, J. (1996). *Biochem. Biophys. Res. Commun.* **227**, 374–379.
Laskowski, R. A., MacArthur, M. W., Moss, D. S. & Thornton, J. M. (1993). *J. Appl. Cryst.* **26**, 283–291.
Lomonte, B., Pizzaro-Cerda, J., Angulo, Y., Gorvel, J. P. & Moreno, E. (1999). *Biochim. Biophys. Acta*, **1461**, 19–26.
Mancheva, I., Aleksiev, B., Kleinschmidt, T. & Braunitzer, G. (1986). *Chemistry of Peptides and Proteins*, edited by W. Voelter, E. Bayer, Y. Ovchinnikov & V. Ivanov, pp. 167–176. Berlin: Walter de Gruyter & Co.
Mancheva, I., Kleinschmidt, T., Aleksiev, B. & Braunitzer, G. (1987). *Biol. Chem. Hoppe-Seyler*, **368**, 343–352.
Maung-Maung-Aye (1990). *Snakes of Medical Importance*, edited by P. Gopalakrishnakone & L. M. Chou, pp. 211–242. National University of Singapore.
Maung-Maung-Thwin, Gopalakrishnakone, P., Yuen, R. & Tan, C. H. (1995). *Toxicon*, **33**, 63–76.
Mounier, C. M., Franken, P. A., Verheij, H. M. & Bon, C. (1996). *Eur. J. Biochem.* **237**, 778–785.
Mounier, C. M., Hackeng, T. M., Schaeffer, F., Faure, G., Bon, C. & Griffin, J. H. (1998). *J. Biol. Chem.* **273**, 23764–23772.
Murshudov, G. N., Vagin, A. A. & Dodson, E. J. (1997). *Acta Cryst.* D**53**, 240–255.
Navaza, J. (1994). *Acta Cryst.* A**50**, 157–166.
Nicholls, A., Sharp, K. A. & Honig, B. (1991). *Proteins*, **11**, 281–296.
Otwinowski, Z. & Minor, W. (1997). *Methods Enzymol.* **276**, 307–326.
Rajashankar, K. R., Tsai, I.-H. & Betzel, Ch. (1999). *Acta Cryst.* D**55**, 1064–1065.
Roussel, A. & Cambillau, C. (1991). *Silicon Graphics Geometry Partners Directory*, pp. 86–89. Mountain View, CA, USA: Silicon Graphics.
Scott, D. (1997). *Venom Phospholipase A_2 Enzymes: Structure, Function and Mechanism*, edited by R. M. Kini, pp. 245–268. Chichester: John Wiley & Sons.
Scott, D. L., Achari, A., Vidal, J. C. & Sigler, P. B. (1992). *J. Biol. Chem.* **267**, 22645–22657.
Sumandea, M., Das, S., Sumandea, C. & Cho, W. (1999). *Biochemistry*, **38**, 16290–16297.
Teng, C. M., Chen, Y. H. & Ouyang, C. (1984). *Biochim. Biophys. Acta*, **786**, 204–212.
Tsai, I.-H., Lu, P.-J. & Su, J.-C. (1996). *Toxicon*, **34**, 99–109.
Verheij, H. M., Boffa, M. C., Rothen, C., Bryckert, M. C., Verger, R. & De Haas, G. H. (1980). *Eur. J. Biochem.* **112**, 25–32.
Wang, Y.-M., Lu, P.-J., Ho, C.-L. & Tsai, I.-H. (1992). *Eur. J. Biochem.* **209**, 635–641.
Zhao, K., Zhou, Y. & Lin, Z. (2000). *Toxicon*, **38**, 901–916.